

## Modified droop control scheme for load sharing amongst inverters in a micro grid

Urvi N. Patel<sup>\*1</sup>, Dipakkumar Gondalia<sup>2a</sup> and Hiren H. Patel<sup>2b</sup>

<sup>1</sup>Department of Electrical Engineering, C.K. Pithawalla College of Engineering & Technology,  
Near Malvan Temple, Dumas Road, Surat, Gujarat, India

<sup>2</sup>Department of Electrical Engineering, Sarvajani College of Engineering & Technology,  
near Athwagate, Surat, Gujarat, India

(Received March 11, 2015, Revised June 5, 2015, Accepted June 9, 2015)

**Abstract.** Microgrid, which can be considered as an integration of various dispersed resources (DRs), is characterized by number of DRs interfaced through the power electronics converters. The microgrid comprising these DRs is often operated in an islanded mode. To minimize the cost, reduce complexity and increase reliability, it is preferred to avoid any communication channel between them. Consequently, the droop control method is traditionally adopted to distribute active and reactive power among the DRs operating in parallel. However, the accuracy of distribution of active and reactive power among the DRs controlled by the conventional droop control approach is highly dependent on the value of line impedance, R/X i.e., resistance to reactance ratio of the line, voltage setting of inverters etc. The limitations of the conventional droop control approach are demonstrated and a modified droop control approach to reduce the effect of impedance mis-match and improve the time response is proposed. The error in reactive power sharing is minimized by inserting virtual impedance in line with the inverters to remove the mis-match in impedance. The improved time response is achieved by modifying the real-power frequency droop using arctan function. Simulations results are presented to validate the effectiveness of the control approach.

**Keywords:** droop control; virtual impedance loop; arctan function; reactive power sharing

---

### 1. Introduction

The advent and march of power electronic converters, have led to the feasibility of microgrid. A microgrid can be thought of as a cluster of distributed resources (DRs), often connected through power electronic interface with the utility. Over the years, several control techniques have been proposed by various researchers to achieve the load sharing and/or to eliminate circulating current among these DRs operating in parallel (Chadorkar *et al.* 1993, Duan *et al.* 1999, Wu *et al.* 2000, Zong 2013, Rowe *et al.* 2013). The various control approaches can broadly be classified into two groups: (i) wired or with communication channel and (ii) wireless or without communication channel.

---

\*Corresponding author, Ph.D. Student, E-mail: [urvi.patel@ckpcet.ac.in](mailto:urvi.patel@ckpcet.ac.in)

<sup>a</sup>M.E. Student, E-mail: [dr.gondaliya@yahoo.com](mailto:dr.gondaliya@yahoo.com)

<sup>b</sup>Professor, E-mail: [hiren.patel@scet.ac.in](mailto:hiren.patel@scet.ac.in)

Wired control approaches include master-slave control, average current sharing control, central type control, and circular chain control (Chadorkar *et al.* 1993, Duan *et al.* 1999, Wu *et al.* 2000, Zong 2013) to achieve the rigid control on the voltage/current for load sharing. However, due to the long communication lines between the distantly placed DRs, such wired control approaches face the issues of stability, reliability, complexity, higher cost and interference by high frequency signals. Wireless control for sharing the power among DRs mainly involves the principle of droop control (Guerrero *et al.* 2004). The real or active power ( $P$ ) and reactive power ( $Q$ ) outputs of the DGs are regulated by controlling the frequency and voltage of the inverter, respectively. The control approach is thus based on  $P-\omega$  and  $Q-V$  relationships and assumes that  $P$  and  $Q$  are decoupled. As the communication lines are absent in this droop control approach, the output voltage references for the DRs are produced by the inverters themselves and hence, chance of interference by noise or high frequency external signals is less.

$P-\omega$  droop control usually gives an accurate sharing of active power. However, the reactive power sharing among the inverter with  $Q-V$  control is sensitive to the output impedance of the inverter and line impedance. Thus, the characteristic of transmission lines also introduces some challenges to the droop control method (Zong 2013). The mismatch in the line impedance can be reduced by adding an inductor in series at the inverter's output terminal (Rowe *et al.* 2013). However, the inductor is heavy, bulky and costly equipment as it must be designed in accordance to the line frequency. To avoid the actual inductance, another option is to emulate the inductor by designing fast voltage control loop (Sabar *et al.* 2000, He and Li 2010, Guerrero *et al.* 2005, 2006, 2007). The loop determines the voltage drop that would have occurred in the actual impedance and accordingly reduces the output voltage of the inverter by appropriately adjusting the reference voltage of the inverter.

The aim of this paper is to target the drawbacks of conventional droop control method and to investigate and devise the wireless control strategy, which gives accurate power sharing and fast response for inverters operating in parallel. The control method here considered consists of three main implements: an inner loop that regulates the output voltage with no steady-state errors, an intermediate loop to program virtual output impedance, and an arctan function implemented by Rowe *et al.* (2013) to achieve better response and settling time and to maintain the system operation within the pre-set boundaries.

This paper begins by introducing the existing theory on power-frequency and reactive power-voltage droop in Section II. The mathematical analysis showing the limitations of the conventional droop control method is included in Section III. Later in section IV, the control scheme to overcome the limitations of the conventional droop control approach is presented. Lastly, the superiority of the proposed control scheme is displayed through the results of the simulation exercises performed using MATLAB/Simulink.

## 2. Conventional droop control method

Fig. 1 shows an AC source as a simplified representation of an inverter. It is connected to an ac bus or load through an inductor  $L_1$ , which represents a purely inductive line. The active power  $P_i$ , reactive power  $Q_i$  and apparent power  $S_i$  supplied by the inverter to the bus/load can be expressed as

$$P_i = \frac{EV}{X} \sin\phi \quad (1)$$

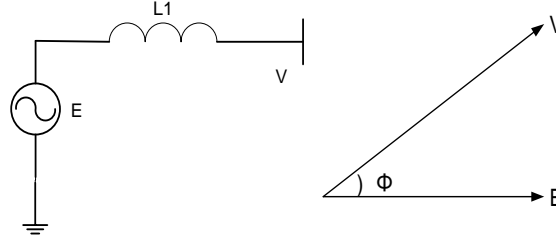


Fig. 1 Simplified representation of a DG connected to a bus

$$Q_i = -\frac{EV \cos \Phi - V^2}{X} \quad (2)$$

$$S_i = P_i + Q_i \quad (3)$$

where  $X$  is the output reactance of an inverter,  $\Phi$  is the phase angle between the output voltage of the inverter and the voltage of the common bus, and  $E$  and  $V$  are the amplitude of the output voltage of the inverter and the common bus, respectively.

From Eq. (1) and Eq. (2), it is evident that the active power  $P_i$  is predominately dependent on the power angle  $\Phi$ , while the reactive power  $Q_i$  mostly depends on the output-voltage amplitude  $E$ . Stated differently;  $P_i$  can be controlled by adjusting the power angle  $\Phi$  and  $Q_i$  can be controlled by regulating voltage  $E$ . However, in a stand-alone system as the units (inverters or DGs) do not know the initial phase values of other units, they use the frequency instead of the power angle or phase angle to control the active power flow. In other words, they employ  $P_i$ - $\omega$  (active power–frequency) droop in place of  $P_i$ - $\Phi$  droop. Thus, by regulating the real and reactive power flows through a power system, the voltage and frequency can be determined. Consequently, most of the wireless-control of paralleled-inverters uses the conventional droop method. The equations representing these droop relation are expressed as

$$\omega = \omega^* - m (P_{oi} - P_i) \quad (4)$$

$$E = E_{ref} - n(Q_{oi} - Q_i) \quad (5)$$

where  $\omega$  is operating frequency of the inverter,  $\omega^*$  is the frequency set point,  $m$  is the frequency droop coefficient,  $P_i$  is the real power of the inverter,  $P_{oi}$  is the real power set point,  $E_{ref}$  is the voltage set point,  $n$  is the voltage droop coefficient, and  $Q_{oi}$  is the reactive power set point. In case, if the output impedances of inverter is highly resistive or if microgrid operate at low voltage then, the reactive power control is dependent on the power angle, while the active power mostly depends on the output-voltage amplitude  $E$ . Consequently, a control scheme based on the  $P$ - $\omega$  and  $Q$ - $V$  droops should be used for inductive impedance, while for resistive impedance  $Q$ - $\omega$  and  $P$ - $V$  droops should be employed. For this reason, it is important to design the output impedance properly in order to improve decoupling between active and reactive power and to avoid the line impedance impact over the power sharing.

### 3. Limitation of conventional droop control method

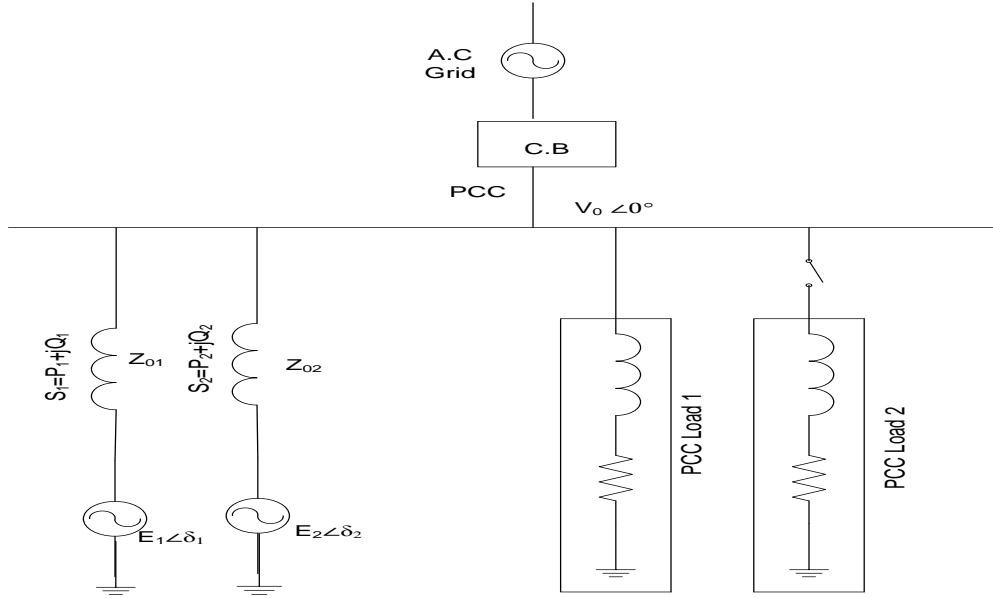


Fig. 2 System configuration consisting of two DGs

Fig. 2 shows two inverters operating in parallel to supply a common load connected at Point of Common Coupling (PCC). The voltage at PCC is  $V_0$  and impedances  $Z_{01}$  and  $Z_{02}$  take care of the mismatch between the inverter output voltages and the output voltage  $V_0$ . Due to the line impedance and a large filter inductance,  $Z_{01}$  and  $Z_{02}$  are considered to be purely inductive. The reference voltages of the two inverters are, respectively

$$V_{r1} = E_1 \sin(\omega_1 t + \delta_1) \quad (6)$$

$$V_{r2} = E_2 \sin(\omega_2 t + \delta_2) \quad (7)$$

where,  $E_1$  and  $E_2$  are the voltage set-points for the inverters. The power ratings of the inverters are

$$S_{1ref} = E_{ref} \times I_{1ref} \quad (8)$$

$$S_{2ref} = E_{ref} \times I_{2ref} \quad (9)$$

where,  $I_{1ref}$  and  $I_{2ref}$  are the rated current of the inverters 1 and 2, respectively.

As stated earlier, because of the inductive impedances,  $Q-E$  and  $P-\omega$  droops are used. The droop coefficients  $n$  and  $m$  are determined by the desired voltage and frequency drops respectively, at the rated active power  $P_{nom}$  and reactive power  $Q_{nom}$  as mentioned by Eqs. (10)-(11).

$$m = \frac{\Delta\omega}{P_{nom}} \quad (10)$$

$$n = \frac{\Delta E}{Q_{nom}} \quad (11)$$

The frequency  $\omega$  is integrated to obtain the phase of the voltage reference. In order for the inverters to share the load in proportional to their power ratings, the droop coefficients of the inverters should be in inverse proportional to their power ratings (Li and Kao 2009), i.e.,  $n_i$  and  $m_i$  should satisfy

$$n_1 S_{1ref} = n_2 S_{2ref} \quad (12)$$

$$m_1 S_{1ref} = m_2 S_{2ref} \quad (13)$$

Hence,  $n_i$  and  $m_i$  also satisfy

$$n_1/m_1 = n_2/m_2 \quad (14)$$

### 3.1 Active power sharing

According to the conventional droop control method, for proportional active load sharing in the steady state, two inverters should work with a same frequency, i.e.,  $\omega_1=\omega_2$ . For the inductive output impedances, the active power accuracy depends on Eq. (13). Indeed, from Eq. (4) for proportional active power sharing following condition must be satisfied.

$$m_1 P_1 = m_2 P_2 \quad (15)$$

Since the coefficients  $m_i$  is chosen to satisfy Eq. (13), it is always ensured that the active power sharing is proportional to their power ratings i.e.

$$\frac{P_1}{S_{1ref}} = \frac{P_2}{S_{2ref}} \quad (16)$$

Alternatively, according to Eq. (1)

$$m_1 \frac{E_1 V_o}{Z_{01}} \sin \delta_1 = m_2 \frac{E_2 V_o}{Z_{02}} \sin \delta_2 \quad (17)$$

If  $\delta_1=\delta_2$  and  $E_1=E_2$ , then

$$\frac{m_1}{Z_{01}} = \frac{m_2}{Z_{02}} \quad (18)$$

### 3.2 Reactive power sharing

The reactive power of the two inverters can be obtained by substituting Eq. (5) into Eq. (2) yielding,

$$Q_i = \frac{E_{ref} \cos \delta_i - V_0}{n_i \cos \delta_i + Z_{oi}/V_0} \quad (19)$$

Substituting Eq. (19) into Eq. (5) the voltage amplitude deviation of the two inverters is

$$\Delta E = E_2 - E_1 = \frac{E_{ref} \cos \delta_i - V_0}{\cos \delta_1 + Z_{oi}/n_1 V_0} - \frac{E_{ref} \cos \delta_i - V_0}{\cos \delta_2 + Z_{oi}/n_2 V_0} \quad (20)$$

It is known from (Li and Kao 2009) that the voltage deviation  $\Delta E$  of the two units leads to

considerable errors in load sharing. Indeed, in order for

$$n_1 Q_1 = n_2 Q_2 \quad \text{or} \quad \frac{Q_1}{S_{1ref}} = \frac{Q_2}{S_{2ref}} \quad (21)$$

to hold, the error  $\Delta E$  should be zero according to Eq. (20). However due to numerical computational errors, disturbances, parameter drifts and component mismatches, it is difficult to observe this condition strictly. This condition is satisfied if

$$\frac{n_1}{Z_{01}} = \frac{n_2}{Z_{02}} \quad \text{and} \quad \delta_1 = \delta_2 \quad (22)$$

In other words,  $n_i$  should be proportional to its output impedance  $Z_{oi}$ . In other words  $Z_{oi}$  should satisfy Eq. (22). Taking Eq. (22) into account, in order to achieve accurate sharing of reactive power, the (inductive) output impedance should be designed to satisfy

$$Z_{01} S_{1ref} = Z_{02} S_{2ref} \quad (23)$$

The per-unit output impedance of inverter  $i$  is

$$\gamma_i = \frac{Z_{oi}}{E_{ref} / I_{iref}} = \frac{Z_{oi} S_{iref}}{(E_{ref})^2} \quad (24)$$

Substituting Eq. (24) into Eq. (23), the condition is equivalent to

$$\gamma_1 = \gamma_2 \quad (25)$$

Thus, in order to achieve accurate proportional power sharing for the conventional droop control scheme, Eq. (25) reveals that the per-unit output impedances of all inverters operated in parallel should be equal (Zhong 2013). If this is not met, then the voltage set-points  $E_i$  are not the same and errors appear in the reactive power sharing. However, this is almost impossible in reality. It is difficult to maintain  $E_1=E_2$  or  $\delta_1=\delta_2$  because of the presence of numerical computational errors, disturbances and noises. It is also difficult to maintain  $\gamma_1=\gamma_2$  because of different feeder impedances, parameter drifts and component mismatches. The reality is that none of these conditions would be met. Hence, a mechanism is needed to achieve an accurate proportional load sharing when such uncertain factors exist

#### 4. Modified droop control

Micro grids, where the per unit impedances are not same, voltage source inverters which are droop controlled using  $P$  v/s  $\omega$  approach may not behave properly as concluded previously. Fig. 3 advocates the control scheme which overcomes the limitations of the conventional control scheme. It incorporates the features of two different approaches: (i) insertion of virtual impedance in series with the feeder resistance to minimize the mismatch in per-unit output impedances of the inverters and (ii) limiting the rate of change of frequency and its excursion by employing arctan function as shown in Fig. 3.

Fig. 4 displays the principle of the modified approach (Tuladhar *et al.* 1997). With a view to match the per unit output impedances of the inverters operating in parallel, the virtual impedance

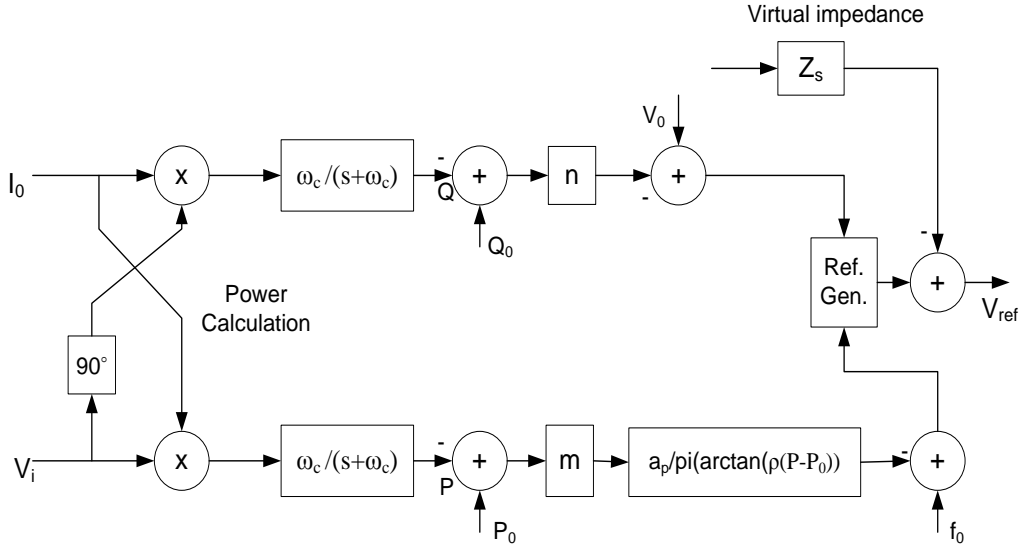


Fig. 3 Modified droop control scheme

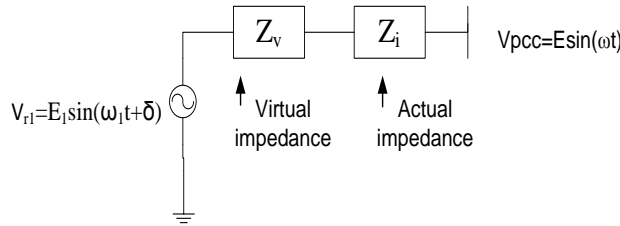


Fig. 4 Adding virtual impedance in conventional system

loop adds virtual impedance in series with the real line impedance to fulfill the condition mentioned in Eq. (18). The virtual impedance creates a “voltage drop” without generating any actual active and/or reactive power losses.

In order to increase the stability of the system, to reduce the impact of circulating currents, and to share linear and nonlinear loads, some approaches introduce virtual impedance into the system by an additional control loop (Guerrero *et al.* 2005, 2006, 2007) that follows the relation

$$V_{ref} = V_{droop} - Zv(s) * I_0 \tag{26}$$

where  $V_{droop}$  is the voltage reference delivered by the droop method and  $Zv(s)$  is the virtual output impedance. The calculation and design of virtual impedances was presented by Guerrero *et al.* (2005).

Fig. 3 shows how the virtual impedance loop is implemented. The virtual voltage drop is calculated using the inverters’ output current. Hence, in this case, the virtual impedance is expected to be added between the inverter and the local load. This allows the inverter’s output impedance to vary virtually.

Insertion of the virtual impedance, as mentioned above, helps in reducing the mis-match of the impedances and overcomes one of the limitations of the conventional droop control. Another,

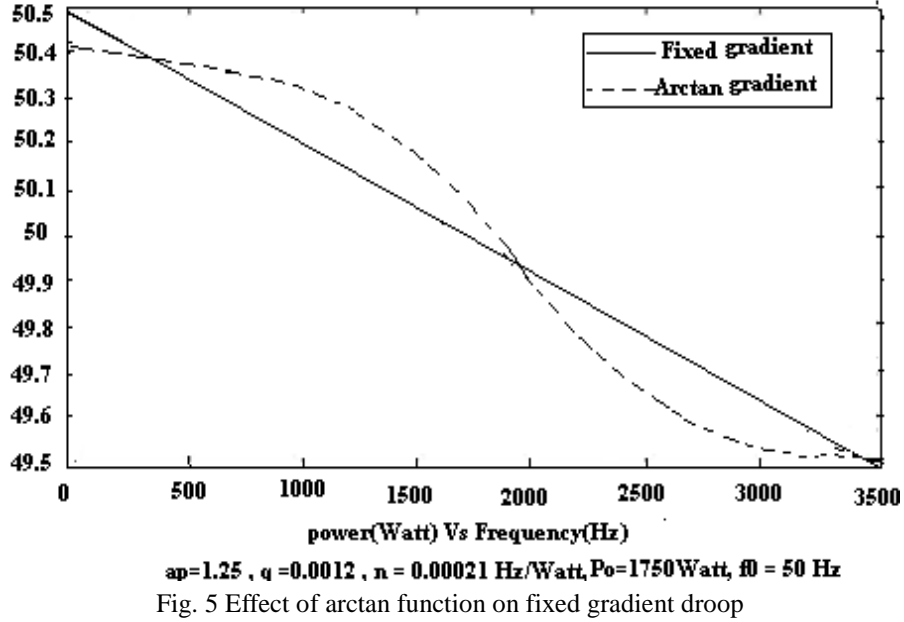


Fig. 5 Effect of arctan function on fixed gradient droop

limitation of the conventional droop control approach is that any excursions in power may cause a rapid change in frequency which causes the DG unit to operate outside the allowed frequency margins. Further, the conventional droop control has the same gradient for the  $P-\omega$  and  $Q-V$  droop for the entire range. According to (Rowe *et al.* 2011), it is observed that higher the  $m$  or  $n$  gradient, faster is the response. Hence, it can be concluded that changing of gradient with the load is required to achieve both these objectives: (i) restricting the frequency within desired range and (ii) faster response.

Arctan based algorithm (Rowe *et al.* 2013) can be applied to overcome these limitations of constant frequency droop and to operate the frequency always within pre-set bounds. In this algorithm dynamic droop adjustments are performed to gain better control whilst implementing frequency and voltage bounding (Rowe *et al.* 2010). These systems basically limit the gradient near the frequency bounds whilst utilising a fixed gradient. Unlike the conventional power frequency droop profile which is inherently limited to have a fixed concavity of zero, the arctan function based droop control allows variance in both gradient and concavity of the power profile. This helps in achieving natural frequency bounding independently from the overall system controller as shown in Fig. 5. The reason for the superior performance with arctan based algorithm is the monotonic increase in the value in the pre-set boundary. In fact, any function (e.g., cube function) that provides a monotonically increasing function for the pre-set boundary can be considered for modification of the power frequency droop profile. However, arctan function is more preferred as it is less complex and involves low computational time.

It has adequate control over the gradient of droop about the power set point, desirable horizontal asymptotes and existing function libraries in most coding languages. The new frequency droop equation is characterised as shown in Eq. (27).

$$f = f_0 - \frac{a_p}{\pi} \times \arctan(\rho(P_i - P_{oi})) \quad (27)$$

Table 1 Ratings, parameters, and control set-points for the system configuration of Fig. 2

Rating of inverter-1 $S_1$	4.5 kVA
Rating of inverter-2 $S_2$	9 kVA
$m_1, m_2$ (Hz/kW)	0.5, 0.25
$n_1, n_2$ (V/kVAR)	10, 5
$P_{01}, P_{02}$ (W)	2000, 4000
$Q_{01}, Q_{02}$ (VAR)	1000, 2000
Load1 ( $\Omega$ )	13.84+j9.23
Load2 ( $\Omega$ ) (Connected at $t=3$ s)	10+j10
$E_{0\ rms}$ (V)	230
$f_0$ (Hz)	50

or equivalently

$$\omega = \omega_0 - 2a_p \arctan(\rho(P_i - P_{0i})) \quad (28)$$

where  $f$  is the operating frequency of the inverter,  $f_0$  is the frequency set point,  $a_p$  is the arctan bounding multiplier, and  $\rho$  is the arctan droop coefficient. By characterising the function it is possible to bind it within the pre-set boundaries. For example, if  $a_p=1$  the frequency is naturally bounded from  $(f_0+0.5)$  Hz to  $(f_0-0.5)$  Hz. By changing  $\rho$  the gradient or concavity is controlled. It is worth to note that under the application of the small angle criteria, the arctan algorithm reduces to the direct  $\delta \propto P$  relationship as the general form of droop given in Eq. (1).

## 5. Simulation results

To demonstrate the effectiveness of the above control strategies, the system shown in Fig. 2 has been simulated in MATLAB/Simulink. The system configuration shown in Fig. 2 is considered to evaluate the various load sharing approaches which include conventional droop control, virtual impedance technique, arctan based droop control and the one presented in Fig. 3. As the operation in islanded mode is much more critical than that of grid connected mode, the comparison is done for islanded mode only. Besides the steady-state performance, the dynamic performances of the control strategy is evaluated by applying a sudden i.e., step change in the load. The ratings of the inverter, droop-coefficients, set-points and details of load taken considered are mentioned in the Table 1.

### *Case-1 : Conventional droop control load sharing with same per unit impedances*

The feeder impedances are considered purely inductive ( $Z_{01}=j3.768\Omega$  and  $Z_{02}=j1.884\Omega=0.5Z_{01}$ ). As the inverter-1 rating is twice the rating of inverter-2, the per unit impedances of these inverters ( $\gamma_1=\gamma_2=0.320$  p.u.) as evident from Eq. (24), are same. The performance with conventional droop control scheme is shown in the Fig. 6(a)-(d). The active and reactive power shared by the inverters till  $t=3$ s (with only load-1 connected at PCC) is 2496W ( $P_1=832$ W,  $P_2=1664$ W= $2P_1$ ) and 1650VAR ( $Q_1=550$ VAR,  $Q_2=1100$ VAR= $2Q_1$ ), respectively and after  $t=3$  s (both load-1 and load-2 connected) is 4233W ( $P_1=2822$ W,  $P_2=1411$ W= $2P_1$ ) and 3513VAR ( $Q_1=1171$ VAR,  $Q_2=2342$ VAR= $2Q_1$ ), respectively. It is observed that the active and reactive power

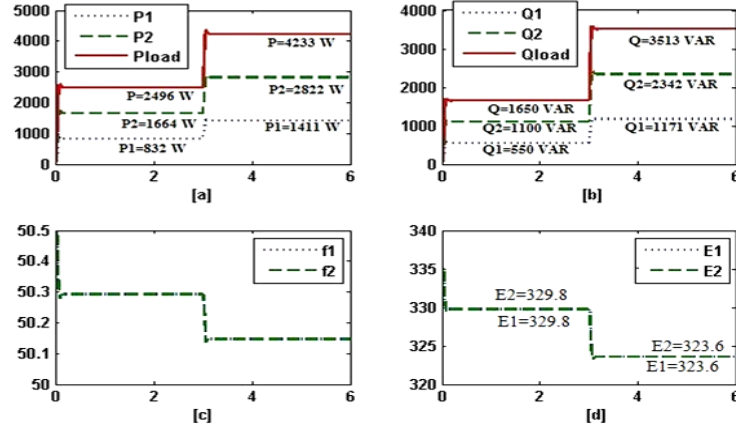


Fig. 6 Power sharing with convention droop control when  $\gamma_1 = \gamma_2$ . (a)-(b) active and reactive power shared by inverters; (c) operating frequency of inverter (d) output voltage of inverter

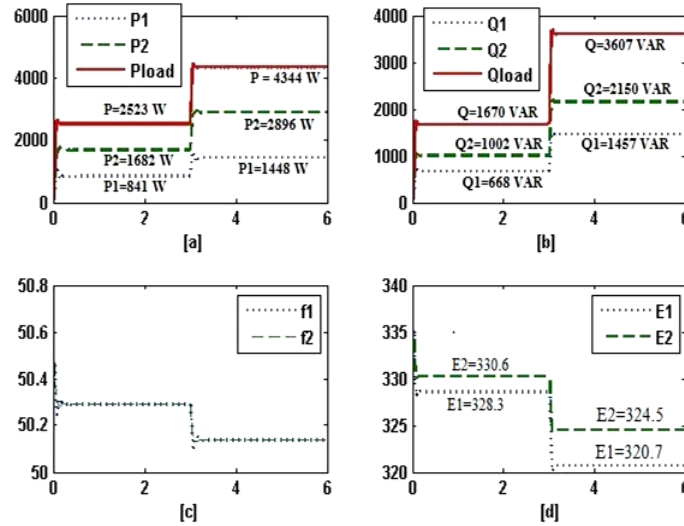


Fig. 7 Power sharing with convention droop control when  $\gamma_1 \neq \gamma_2$ . (a)-(b) active and reactive power shared by inverters; (c) operating frequency of inverter (d) output voltage of inverter

sharing amongst the inverters are exactly in the ratio of their power (kVA) ratings i.e.,  $S_1/S_2$ . Fig. 6(d) also shows that voltage deviation  $\Delta E = E_2 - E_1$  is zero.

#### Case-II: Conventional droop control load sharing with unequal per unit impedances

Fig. 7 (a)-(d) shows the performance of the conventional droop control when per unit impedance of the feeder-2 is same as in Case-1 ( $Z_{02} = j1.884 \Omega$ ) while per unit impedance of feeder-1 is changed to  $Z_{01} = j2.512 \Omega$ . Thus, the per unit impedance of the two feeders ( $\gamma_1 = 0.2136$  and  $\gamma_2 = 0.320$  p.u) are no longer same. It exhibits that the active power supplied by the inverters still follows the relation  $P_2 = 2P_1$  confirming the equal active power sharing even when the per-unit

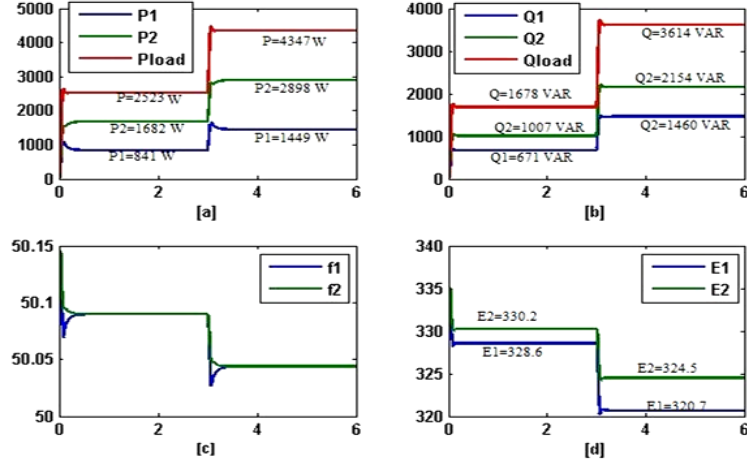


Fig. 8 Performance with droop control having virtual impedance loop when  $\gamma_1 \neq \gamma_2$ : (a); (b) active and reactive power shared by the inverters, respectively; (c) operating frequency of the inverters; (d) amplitude of output voltage of the inverters

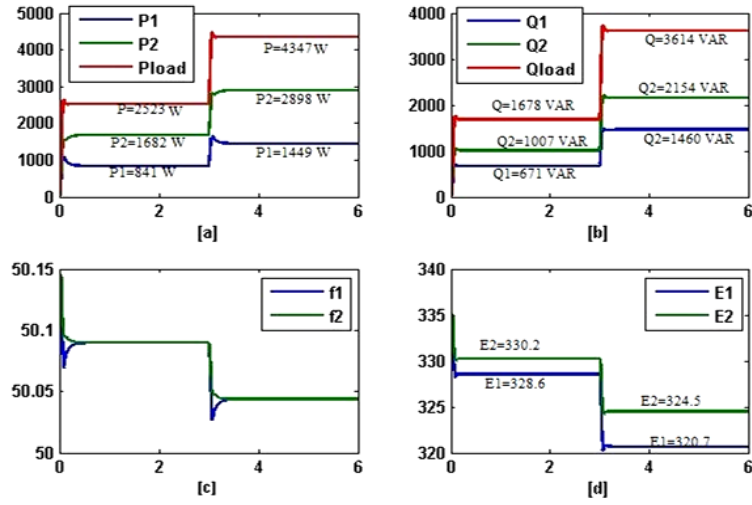


Fig. 9 Performance with arctan function based modified droop control and  $\gamma_1 \neq \gamma_2$ : (a),(b) active and reactive power shared by the inverters, respectively; (c) of the inverters; (d) amplitude of output voltage of the inverters operating frequency

impedance of the feeders are not equal. However, due to the mismatch in the values of per unit impedances, it is clearly observed that the sharing of reactive power no longer follows the relation  $Q_2=2Q_1$ . Thus, the mis-match in per-unit impedances of the feeders introduces error in the reactive power sharing but not in the active power sharing. The errors in active and reactive power sharing by the inverters are defined as under

$$e_{Pi} = \frac{P_i^* - P_i}{P_i^*} \times 100\% \quad (29)$$

$$e_{Qi} = \frac{Q_i^* - Q_i}{Q_i^*} \times 100\% \quad (30)$$

where  $P_i^*$  is the active power and  $Q_i^*$  is the reactive power supplied by the  $i^{\text{th}}$  inverter when both the inverters share the active and reactive power exactly in proportion to their ratings. The reactive power sharing errors,  $e_{Q1}$  and  $e_{Q2}$ , for the inverters 1 and 2 are -19.99% and 9.99% till  $t=3$  s and -21.18% and 10.59% after  $t=3$  s. In addition it can be observed from Fig. 8(d) that unlike, the Case-I voltage deviation  $\Delta E = E_2 - E_1 = 2.3\text{V}$  is also not zero.

**Case -III: Virtual impedance based droop control under the conditions  $\gamma_1 \neq \gamma_2$**

The inverters per unit impedances are maintained at the same values,  $Z_{01} = j2.512\Omega$  and  $Z_{02} = j1.884\Omega$ , as in case II ( $\gamma_1 = 0.2136$  p.u. and  $\gamma_2 = 0.320$  p.u.). To minimize the effect of mis-match in the per unit impedances, virtual impedance  $Z_V$  is added in series with  $Z_{01}$ . The virtual inductive impedance loop is employed to achieve the matching of impedances and thereby improve power sharing, especially the reactive power shared by the inverters. Fig. 8 reveals that the insertion of virtual impedance minimizes the error in the reactive power sharing and deviation in the output voltage of the inverters. The errors  $e_{Q1}$  and  $e_{Q2}$  with the virtual impedance is 6.13% and -3.07% till  $t=3$  s and mere 0.4% and -0.2% after  $t=3$  s. Fig. 8(d) shows that the deviation in output voltage has also reduced significantly to 0.1V. However, as shown in Fig. 8(c) this has been achieved at the cost of higher settling time and oscillatory response at the starting ( $t=0$  s) and at the time of step change in the load ( $t=3$  s).

**Case-IV: Arctan function based modified droop control for load sharing under the conditions  $\gamma_1 \neq \gamma_2$**

Fig. 9 shows the performance with the arctan function based droop control. The arctan function is implemented in power-frequency droop. The impedances of feeders are maintained at the same values,  $Z_{01} = j2.512\Omega$  and  $Z_{02} = j1.884\Omega$  (i.e., per unit impedances  $\gamma_1 = 0.2136$  p.u. and  $\gamma_2 = 0.320$  p.u.), as in case II. It is observed that the active power is shared in the proportion to the ratings of the

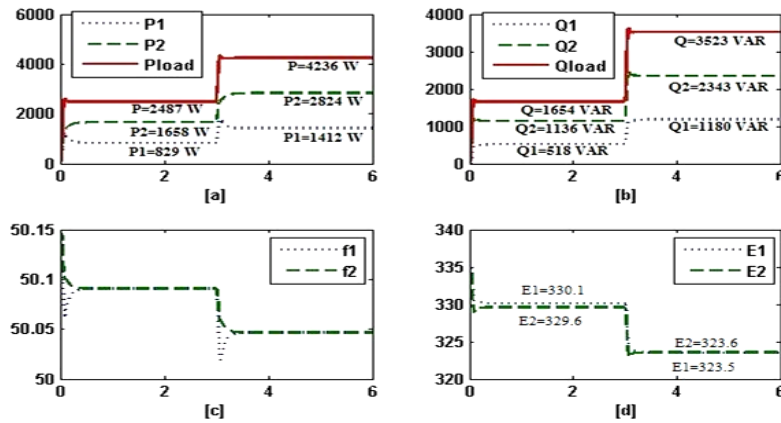


Fig. 10 Performance with both arctan function and virtual impedance based modified droop control for  $\gamma_1 \neq \gamma_2$ : (a)-(b) active and reactive power shared by the inverters, respectively; (c) operating frequency of the inverters; (d) amplitude of output voltage of the inverters

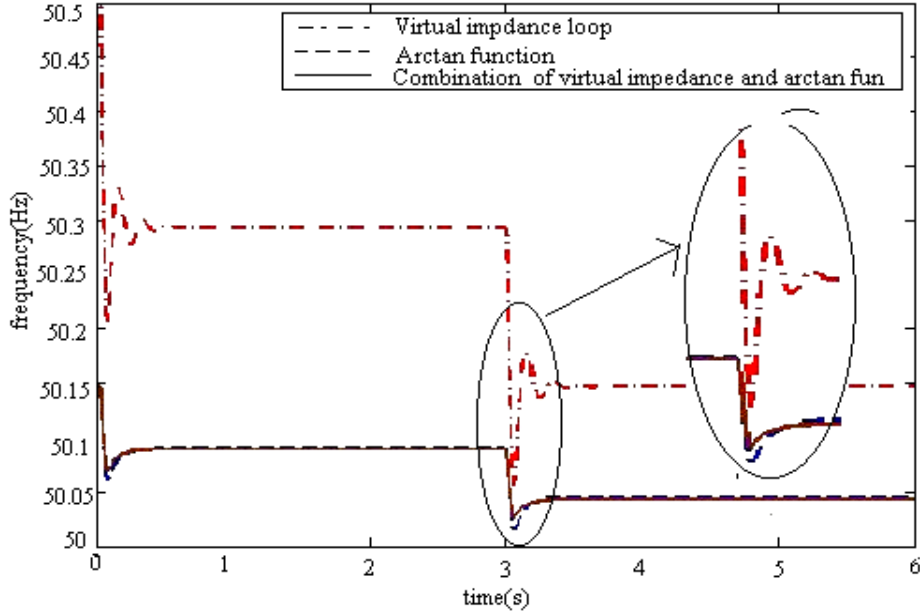


Fig. 11 Frequency response for the cases III-V

Table 2 Comparison of steady state and transient performance with different control approaches

Control Approach	$e_{Q1}$ (%)	$e_{Q2}$ (%)	$t_s$ (s)
Conventional droop with mismatch impedance	21.18	10.59	0.2
Conventional droop with virtual impedance loop	0.4	-0.2	0.5
Modified droop with Arctan function	-21.2	10.6	0.10
Modified droop control with Arctan function and Virtual impedance loop	0.4	-0.2	0.06

inverter. However, reactive power sharing is not in the ratio of the ratings of the inverters. The reactive power sharing errors,  $e_{Q1}$  and  $e_{Q2}$ , for the inverters 1 and 2 are -19.96% and 9.99% till  $t=3$  s and -21.2% and 10.6 % after  $t=3$  s. In addition it can be observed from Fig. 9(d) that unlike, the Case-1 voltage deviation  $\Delta E=E_2-E_1 \neq 0$ . However, Fig. 9(c) reveals that the insertion of arctan function minimizes the frequency oscillation and improves transient response.

#### Case-V: Load sharing with droop modified with both arctan function and virtual impedance loop

In this case the power-frequency droop is modified with the arctan function as in case-IV. Additionally, the virtual impedance loop is incorporated in the control scheme. The feeder impedances are maintained at the same values  $Z_{01}=j2.512\Omega$  and  $Z_{02}=j1.884\Omega$  (i.e., per unit impedances  $\gamma_1=0.2136$  p.u. and  $\gamma_2=0.320$  p.u.) as in cases II-IV.

Fig. 10 shows that the active and reactive power sharing is accurate and the response time and settling time are improved. Fig. 10(b) reveals that the insertion of virtual impedance minimizes the error in the reactive power sharing and deviation in the output voltage of the inverters and Fig. 10(c) shows that the frequency response is improved due to the arctan function. The errors  $e_{Q1}$  and

$e_{O2}$  with the virtual impedance is 6.13% and -3.07% till  $t=3$  s and mere 0.4% and -0.2% after  $t=3$  s. Fig. 10(d) shows that the deviation in output voltage has also reduced significantly 0.1V. So, advantages of both arctan function and virtual impedance can be achieved by combining the features of these two methods with the conventional droop control concept.

Fig. 11 compares the response of frequency for the cases III-V. It can be observed that the control scheme which incorporates the features of both arctan function based control and virtual impedance loop based control give better steady state and good transient response. Table 2 summarizes the steady state and transient performance of the system with different control approaches in response to the load change at  $t=3$  sec. The response is quantified in terms of  $e_{O1}$ ,  $e_{O2}$  and settling time  $t_s$ , for  $\gamma_1=0.2136$  p.u. and  $\gamma_2=0.320$  p.u.

## 6. Conclusions

With the conventional droop control approach, it is must to maintain the same voltages set-points and per-unit impedance of the inverters, to ensure active and reactive power sharing in proportion to the rating of the inverters operating in parallel. In case of the violation of above, the inverters do share the active power in proportion to their ratings, but not the reactive power. The modified control scheme that encompasses the feature of both virtual impedance control and arctan based modified droop control not only overcomes this limitation but also exhibits superior response under transient conditions. As the gradient of modified droop (based on arctan function) near the extremes/limit of the range is low, the rate of change of frequency and its overshoot are less than that in case of conventional droop control. The results confirm that the proposed approach performs accurately even when the output per-unit impedance do not match ( $\gamma_1 \neq \gamma_2$ ). However, it must be ensured that  $\frac{n_1}{m_1} = \frac{n_2}{m_2}$ .

## References

- Broeck, H.V. and Boeke, U. (1998), "A simple method for parallel operation of inverters", *Telecommunications Energy Conference, INTELEC*, Twentieth International, 143-150.
- Chandorkar, M.C., Divan, D.M. and Adapa, R. (1993), "Control of parallel connected inverters in standalone ac supply systems", *IEEE Trans. Ind. Appl.*, **29**(1), 136 - 143.
- Duan, S., Meng, Y., Xiong, J., Kang, Y. and Chen, J. (1999), "Parallel operation control technique of voltage source inverters in UPS", *IEEE International Conference on Power Electronics and Drive Systems, PEDS'99*, Hong Kong.
- Guerrero, J.M., Matas, J., García De Vicuña, L., Castilla, M. and Miret, J. (2007), "Decentralized control for parallel operation of distributed generation inverters using resistive output impedance", *IEEE Trans. Ind. Electron.*, **54**(2), 994-1004.
- Guerrero, J.M., Matas, J., Vicuña, D., García, L., Castilla, M. and Miret, J. (2006), "Wireless-control strategy for parallel operation of distributed generation inverters", *IEEE Trans. Ind. Electron.*, **53**(5), 1461- 1470.
- Guerrero, J.M., Vicuña, D., García, L., Matas, J., Castilla, M. and Miret, J. (2005), "Output impedance design for parallel-connected UPS inverters with wireless load sharing control", *IEEE Trans. Ind. Electron.*, **52**(4), 1126-1135.
- Guerrero, J.M., Vicuña, D., García, L., Matas, J., Castilla, M. and Miret, J. (2004), "A wireless controller to enhance dynamic performance of parallel inverters in distributed generation systems", *IEEE Trans. Power*

- Electron.*, **9**, 1205-1213.
- He, J. and Li, Y.W. (2010), "Analysis, design, and implementation of virtual impedance for power electronics interfaced distributed generation", *IEEE Trans. Ind. Appl.*, **47**(6), 2525-2538.
- Li, Y.W. and Kao, C.N. (2009), "An accurate power control strategy for power electronics interfaced distributed generation units operating in a low voltage multibus microgrid", *IEEE Trans. Power Electron.*, **24**(12), 2977-2988.
- Matas, J., Castilla, M., de Vicuña, L.G., Miret, J. and Vasquez, J.C. (2010), "Virtual impedance loop for droop-controlled single-phase parallel inverters using a second-order general-integrator scheme", *IEEE Trans. Power Electron.*, **25**(12), 2993-3002.
- Rowe, C., Summers, T.J. and Betz, R. (2010), "Arctan power frequency droop for power electronics dominated microgrids", *Proc. Australas. Univ. Power Eng. Conf.*, 1-6.
- Rowe, C., Summers, T.J., Betz, R. and Cornforth, D. (2011), "Small signal stability analysis of arctan power frequency droop", *Proc. Power Electron. Drive Syst. Conf.*, 787-792.
- Rowe, C., Summers, T.J. and Betz, R. and Cornforth, D. and Moore, T.G. (2013), "Arc tan power-frequency droop for improved microgrid stability", *IEEE Trans. Power Electron.*, **28**(8), 3747-3759.
- Sabar, F.A., Mohammadi, H., Ketabi, A. and Masoud, S. (2000), "Control of parallel inverters in distributed AC power systems with consideration of line impedance effect", *IEEE Trans. Ind. Appl.*, **36**(1)131-138.
- Tuladhar, A., Jin, H., Unger, T. and Mauch, K. (1997), "Parallel operation of single phase inverter modules with no control interconnections", *Proc. 12th Annu. APEC*, **1**, 94-100.
- Wu, T.F., Chen, Y.K. and Huang, Y.H. (2000), "3C strategy for inverters in parallel operation achieving an equal current distribution", *IEEE Trans. Ind. Electron.*, **47**(2), 273-281.
- Zhong, Q.C. (2013), "Robust droop controller for accurate proportional load sharing among inverters operated in parallel", *IEEE Trans. Ind. Electron.*, **60**(4), 3747-3459.